

Analysis and Circuit Modeling of APDs

A. Ahadpour Shal, A. Ghadimi, A. Azadbar

Abstract—In this paper a new method for increasing the speed of SAGCM-APD is proposed. Utilizing carrier rate equations in different regions of the structure, a circuit model for the structure is obtained. In this research, in addition to frequency response, the effect of added new charge layer on some transient parameters like slew-rate, rising and falling times have been considered. Finally, by trading-off among some physical parameters such as different layers widths and droppings, a noticeable decrease in breakdown voltage has been achieved. The results of simulation, illustrate some features of proposed structure improvement in comparison with conventional SAGCM-APD structures.

Keywords—Optical communication systems (OCS), Circuit modeling, breakdown voltage, SAGCM APD

I. INTRODUCTION

THE performance of OCS applied photodiodes has been improved by amending of used materials qualities and device structure developments [1]. Avalanche photodiodes (APDs) in comparison with the PIN photodiodes have the internal gain which causes higher detection sensitivity [2]. In APDs, separation of absorption (A) and multiplication layers (M) causes a lower noise and lower dark current [3] so that, achieving better performance, a narrow bandgap material is used in absorption layer and a wide bandgap one is utilized in multiplication layer. Also, a high electric field applied to the multiplication layer to increase the gain-bandwidth product, and this can be achieved better by using a charge sheet layer of high doping density (C) [4]. In recent years, various structures of the APDs have been presented, in which, absorption and multiplication layers are separated, so that, only one type of carrier is transported into the multiplication region, which reduces the multiplication noise. Also, thinner the multiplication region width and lower breakdown voltage of APDs are most important features of modern OCS and other applications [5]. High-performance APDs are achieved by using separated absorption, grading, charge and multiplication layers (SAGCM) [6]. The gain-bandwidth characteristic is one of the most important parameter of the APDs. The gain-bandwidth characteristic is one of the most important parameter of the APDs and its high quantities, makes it available to work in high bit rates and defines these systems future development stages.

Alireza Ahadpour Shal is with the Department of Electrical Engineering, Lahijan Branch, Islamic Azad University, Lahijan, Iran (phone: 0098-141-2229081; fax: 0098-141-2228701; e-mail: a_ahadpour@liau.ac.ir).

A. Ghadimi is with the Department of Electrical Engineering, Lahijan Branch, Islamic Azad University, Lahijan, Iran (phone: 0098-141-2229081; fax: 0098-141-2228701; e-mail: ghadimi@liau.ac.ir).

A. Azadbar is with the Department of Electrical Engineering, Lahijan Branch, Islamic Azad University, Lahijan, Iran (phone: 0098-141-2229081; fax: 0098-141-2228701; e-mail: azadbar@liau.ac.ir).

In all pervious works APDs speed criterion was gain-bandwidth product and transient response parameters in term of slew-rate haven't been considered. A few analysis and circuit models for APDs with separation of absorption and multiplication layers have been reported [7, 8, 9, 10], and also there are only a few attempts to study the frequency and impulse response of the APDs.

In this work, to achieve higher performance device, a new thin charge layer, have been added between absorption and grading layers to obtain a new structure which can be called SAGCM. Furthermore, in addition to gain-bandwidth product consideration, frequency response and effective speed parameters such as slew rate, fall time and rise time have been studies as transient time response. All results show a great improvement in comparison with its predecessors. Furthermore, breakdown voltage of device has been reduced by controlling the electric field in multiplication layer which is the most important features of photo detector.

In section 2 and 3, novel SAGCM structure, its electric field profile and different layers equations and its circuit model are presented. Simulation results and their comparisons with other conventional SAGCM structures are shown in section 4 and finally, conclusion is provided in section 5.

II. ELECTRIC FIELD PROFILE AND RATE EQUATIONS

Adding the charge layer causes an increase in primary transport speed of generated optical carriers from absorption layer to multiplication layer. We name the new charge layer (c_1) and the charge layer between grading and multiplication layer (c_2). Assume that the light illuminates from p+ region to device so that the current of device has 2 parts; diffusion current which is related to minority carriers in p and n regions and drift current which is created in absorption and multiplication region. Electric field in absorption, first charge layer and grading region is assumed to be uniform also because of strong electric field in multiplication region and a part of second charge layer, impact ionization phenomenon is considered therein in addition, depletion region width in n+ and p+ layer is neglected. We suppose electric field in the second charge region and multiplication region can be assumed fully depleted and modeled by consecutive progressive steps.

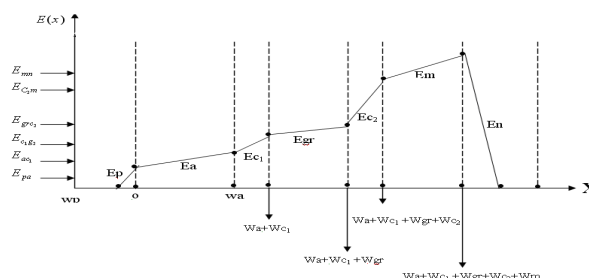


Fig. 1 Electric field of Structure

Electric field profile, base on structural parameters and length of different layers can be described by following equations.

$$E_p(x) = \frac{qN_p}{\epsilon_p} (x + w_p) \quad w_p \leq x \leq 0 \quad (1)$$

$$E_{C_1}(x) = \frac{qN_p}{\epsilon_p} w_p + \frac{qN_a}{\epsilon_a} w_a + \frac{qN_{c1}}{\epsilon_{c1}} (x - w_a) \quad (2)$$

$$E_a(x) = \frac{qN_p}{\epsilon_p} w_p + \frac{qN_a}{\epsilon_a} (x - 0) \quad 0 \leq x \leq wa \quad (3)$$

$$wa \leq x \leq wa + wc_1$$

$$E_{gr}(x) = \frac{qN_p}{\epsilon_p} w_p + \frac{qN_a}{\epsilon_a} w_a + \frac{qN_{c1}}{\epsilon_{c1}} w_{c1} + \frac{qN_{gr}}{\epsilon_{gr}} (x - w_a - w_{c1}) \quad (4)$$

$$wa + wc_1 \leq x \leq wa + wc_1 + w_{gr}$$

$$wa + wc_1 + w_{gr} \leq x \leq wa + wc_1 + w_{gr} + wc_2$$

$$E_{c_2}(x) = \frac{qN_p}{\epsilon_p} w_p + \frac{qN_a}{\epsilon_a} w_a + \frac{qN_{c1}}{\epsilon_{c1}} w_{c1} + \frac{qN_{gr}}{\epsilon_{gr}} w_{gr} + \frac{qN_{c2}}{\epsilon_{c2}} (x - wa - wc_1 - w_{gr}) \quad (5)$$

$$E_m(x) = \frac{qN_p}{\epsilon_p} w_p + \frac{qN_a}{\epsilon_a} w_a + \frac{qN_{c1}}{\epsilon_{c1}} w_{c1} + \frac{qN_{gr}}{\epsilon_{gr}} w_{gr} + \frac{qN_{c2}}{\epsilon_{c2}} w_{c2} + \frac{qN_m}{\epsilon_m} (x - wa - w_{c1} - w_{gr} - w_m) \quad (6)$$

$$E_n(x) = \frac{qN_p}{\epsilon_p} w_p + \frac{qN_a}{\epsilon_a} w_a + \frac{qN_{c1}}{\epsilon_{c1}} w_{c1} + \frac{qN_{gr}}{\epsilon_{gr}} w_{gr} + \frac{qN_{c2}}{\epsilon_{c2}} w_{c2} + \frac{qN_m}{\epsilon_m} w_{c2} + \frac{qN_n}{\epsilon_n} (x - wa - w_{c1} - w_{gr} - w_m - w_n) \quad (7)$$

$$wa + wc_1 + w_{gr} + wc_2 + w_m \leq x \leq wa + wc_1 + w_{gr} + wc_2 + w_m + w_n$$

Carrier rate equations for this approximate model in various regions are;

$$p^+ \text{ region} : \frac{dn_{p^+}}{dt} = N_{Gp} - \frac{n_{p^+}}{\tau_{mp}} - \frac{In}{q} \quad \& \quad N_{Gp} = 0 \quad (8)$$

$$n^- \text{ A region} : \frac{dp_a}{dt} = P_{Ga} - \frac{p_a}{\tau_{pra}} - \frac{p_a}{\tau_{pta}} + \frac{In}{q} \quad (9)$$

$$n \text{ C}_1 \text{ region} : \frac{dp_{c1}}{dt} = P_{Gc1} - \frac{p_{c1}}{\tau_{prc1}} - \frac{p_{c1}}{\tau_{ptc1}} \quad (10)$$

$$n \text{ G region} : \frac{dp_g}{dt} = P_{Ggr} - \frac{p_{gr}}{\tau_{prgr}} - \frac{p_{gr}}{\tau_{ptgr}} \quad (11)$$

n C₂ region :

$$\left\{ \begin{aligned} \frac{dP_{C_{21}}}{dt} &= P_{G_{C_{21}}} + (\alpha_{C_{21}} \cdot v_{nc_{21}} + \beta_{C_{21}} \cdot v_{pc_{21}}) \cdot P_{C_{21}} - \frac{P_{C_{21}}}{\tau_{prc_{21}}} - \frac{P_{C_{21}}}{\tau_{ptc_{21}}} \\ \frac{dP_{C_{22}}}{dt} &= P_{G_{C_{22}}} + (\alpha_{C_{22}} \cdot v_{nc_{22}} + \beta_{C_{22}} \cdot v_{pc_{22}}) \cdot P_{C_{22}} - \frac{P_{C_{22}}}{\tau_{prc_{22}}} - \frac{P_{C_{22}}}{\tau_{ptc_{22}}} \\ \frac{dP_{C_{23}}}{dt} &= P_{G_{C_{23}}} + (\alpha_{C_{23}} \cdot v_{nc_{23}} + \beta_{C_{23}} \cdot v_{pc_{23}}) \cdot P_{C_{23}} - \frac{P_{C_{23}}}{\tau_{prc_{23}}} - \frac{P_{C_{23}}}{\tau_{ptc_{23}}} \\ \frac{dP_{C_{24}}}{dt} &= P_{G_{C_{24}}} + (\alpha_{C_{24}} \cdot v_{nc_{24}} + \beta_{C_{24}} \cdot v_{pc_{24}}) \cdot P_{C_{24}} - \frac{P_{C_{24}}}{\tau_{prc_{24}}} - \frac{P_{C_{24}}}{\tau_{ptc_{24}}} \end{aligned} \right. \quad (12)$$

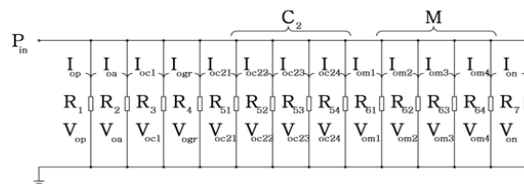
n M region :

$$\left\{ \begin{aligned} \frac{dP_{m1}}{dt} &= P_{G_{m1}} + (\alpha_{m1} \cdot v_{nm1} + \beta_{m1} \cdot v_{pm1}) \cdot P_{m1} - \frac{P_{m1}}{\tau_{prm1}} - \frac{P_{m1}}{\tau_{ptm1}} + \frac{I_{p1}}{q} \\ \frac{dP_{m2}}{dt} &= P_{G_{m2}} + (\alpha_{m2} \cdot v_{nm2} + \beta_{m2} \cdot v_{pm2}) \cdot P_{m2} - \frac{P_{m2}}{\tau_{prm2}} - \frac{P_{m2}}{\tau_{ptm2}} + \frac{I_{p2}}{q} \\ \frac{dP_{m3}}{dt} &= P_{G_{m3}} + (\alpha_{m3} \cdot v_{nm3} + \beta_{m3} \cdot v_{pm3}) \cdot P_{m3} - \frac{P_{m3}}{\tau_{prm3}} - \frac{P_{m3}}{\tau_{ptm3}} + \frac{I_{p3}}{q} \\ \frac{dP_{m4}}{dt} &= P_{G_{m4}} + (\alpha_{m4} \cdot v_{nm4} + \beta_{m4} \cdot v_{pm4}) \cdot P_{m4} - \frac{P_{m4}}{\tau_{prm4}} - \frac{P_{m4}}{\tau_{ptm4}} + \frac{I_{p4}}{q} \end{aligned} \right. \quad (13)$$

$$n^+ \text{ region} : \frac{dP_{n^+}}{dt} = P_{Gn} - \frac{P_{n^+}}{\tau_{pn}} - \frac{I_p}{q} \quad \& \quad P_{Gn} = 0 \quad (14)$$

III. EQUIVALENT CIRCUIT MODEL OF STRUCTURE

To achieve circuit model of device, firstly, we need change the physical parameters to circuit parameters. Thus, we employ a constant capacitor value, C₀, to change charge to voltage. By dividing carrier charge of regions into C₀, potential of carriers in each region will obtain. Take in to accounting different potentials, carrier combination process and also photo generation rate; we can calculate the equal resistors of regions. With parameters in obtained equations we can rewrite the equations and exploit the circuit parameters. circuit model of this structure is shown in Fig. 2.



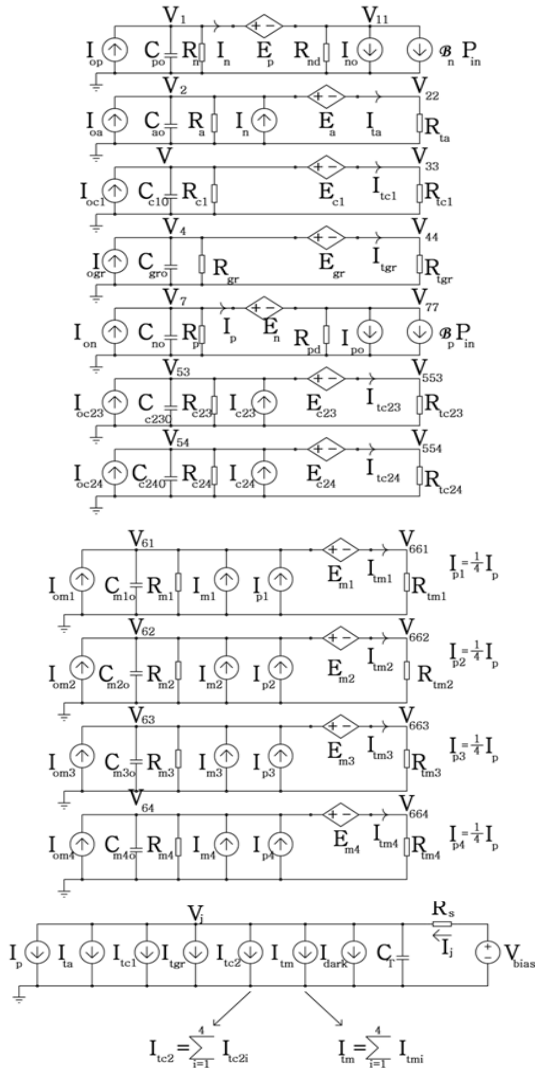


Fig. 2. Circuit model of structure

IV. SIMULATION RESULT

Several simulations have been done to confirm our proposed structure. Fig. 3. Shows that by increasing M layer width device gains will increase. Also a GBW growth of 26% is attained.

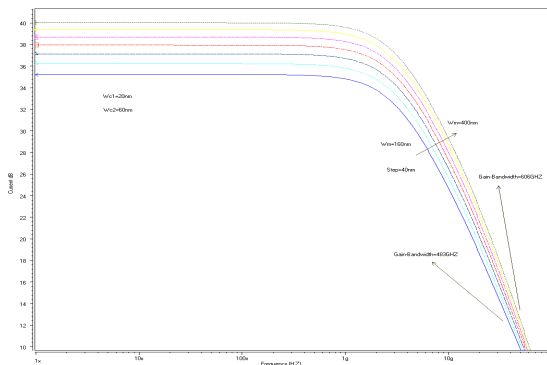


Fig. 3 Gain vs BW in several thicknesses of M

Fig. 4. illustrate that in smaller M layer thicknesses, the lower breakdown voltage can be achieved. By increasing the M layer width, breakdown voltage increases. As it mentioned in Reference [11], for SAGCM with 0.4um multiplication layer thickness, a breakdown voltage of 60(v) is obtained whereas in this structure, with 0.5um multiplication layer thickness, the breakdown voltage is around 44.2(v).

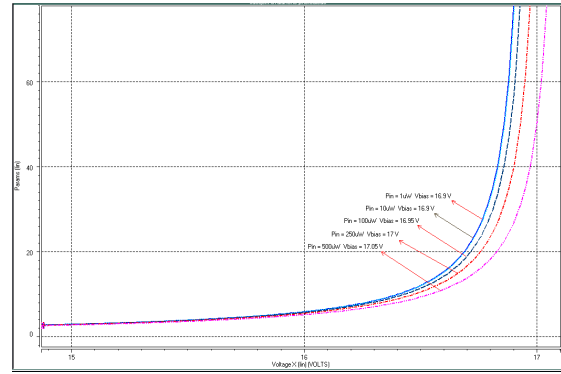


Fig. 4 Gain vs Voltage in several thicknesses of M

Fig. 5 show response to optical pulse and various M layer thickness which shows slew rate increment by C₁ thickness that can be seen in Figure 6.

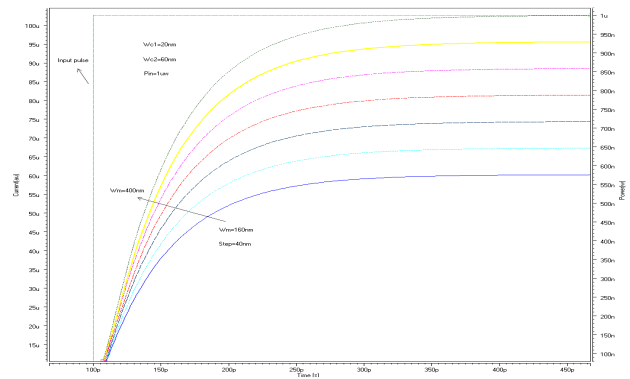


Fig. 5 response for several M layer thicknesses

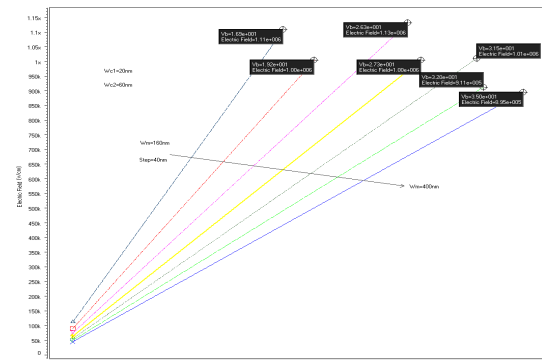


Fig. 6 Slew-rate of APD for various charge layer thicknesses

It can be seen in Fig. 6. that, with the thicker C_1 layer, the output current increases and cause a higher gain. Also With increasing this thickness, the output current has faster response in the respect of more photo carriers' generation in a time span that can be explained by slow rate.

The detector's rising and falling time has suitable response because of C_1 layer existence and their electric fields control. By adding C_1 layer and controlling its electric field, Rising time in comparison with conventional SAGCM improves and it's a convenient criterion of detector speed increase. The falling time depends on C_2 layer thickness and its electric field control. The C_2 layer causes faster transferring of photo carriers from A layer to M layer and by controlling the charge in C_1 layer this structure can be tunable

This is an advantage of this structure in comparison with conventional SAGCM structures.

V. CONCLUSION

A new structure of APDs by adding a layer between absorption and multiplication region has been introduced. It was shown that this additional layer causes significant improvement in GBW product. Simulation results show 23% improvement in gain-bandwidth product and decreases breakdown voltage in comparison with other conventional SAGCM structures. Also, a circuit model was derived from obtained equations which were obtained and developed from carrier rate equations based on assumption of non uniform electric field in C_2 and M regions.

ACKNOWLEDGEMENT

This research is financially supported by Islamic Azad University of Lahijan. The authors would like to appreciate Professor V. Ahmadi for his support and encouragement on this project.

REFERENCES

- [1] F. Ma, S. Wang, and X. Li; "Monte Carlo simulation of low noise avalanche photodiodes with heterojunction," *Appl. Phys. Lett.*, vol. 92, no. 2, pp. 4791-4795, 2002.
- [2] G.Wang, T.Tokumitsu, I.Hanawa, Y.Yoneda, K.Sato, and M.Kobayashi, "A time-delay equivalent-circuit model of ultrafast p-i-n photodiodes" *IEEE Trans. Microw. Theory Tech.*, vol. 51, no. 4, pp. 1227-1233, Apr. 2003.
- [3] F. Ma, S. Wang, and X. Li; "Monte Carlo simulation of low noise avalanche photodiodes with heterojunction," *Appl. Phys. Lett.*, vol. 92, no. 2, pp. 4791-4795, 2002.
- [4] F. Barzegar, M. H. Sheikhi, "A New Physical Modeling for Multiquantum Well Structure APD Considering Nonuniformity of Electric Field in Active Region", *International Journal of Electrical and Electronics Engineering*, vol.2, no. 1, pp. 45-52, 2009
- [5] N.Duan, S.Wang, X.G.Zheng, X.Li, LiNing, J.C.Campbell, C.Wang, and L.A.Coldren, "Detrimental effect of impact ionization in the absorption region on the frequency response and excess noise performance of InGaAs-InAlAs SACM avalanche photodiodes," *IEEE J. Quant. Electron.*, vol. 41, no. 4, pp. 568-572, Apr. 2005.
- [6] Y. Zhao, S. He, "Multiplication characteristics of InP/InGaAs avalanche photodiodes with a thicker charge layer," *Optical Communications* 265, pp. 476-480, 2006.
- [7] S. An, M. J. Deen, "Low-frequency noise in single growth planar separate absorption, grading, charge, and multiplication avalanche photodiodes," *IEEE Trans. Electron. Dev.* 47, pp. 537-543 (2000).
- [8] L. E. Tarof, "Planar InP/InGaAs avalanche photodetector with a gain-bandwidth product in excess of 100 GHz," *Electron. Lett.* 27, pp. 34-36 (1991).

- [9] H. Nie, O. Baklenov, P. Yuan, C. Lenox, B. G. Streetman, and J. C. Campbell, "Quantum-dot resonant-cavity separate absorption, charge, and multiplication avalanche photodiode operating at 1.06 μm ," *IEEE Photon. Technol. Lett.* 10, pp. 1009-1011 (1998).
- [10] C. Lenox, H. Nie, P. Yuan, G. Kinsey, A. L. Holmes, Jr., B. G. Streetman, and J. C. Campbell, "Resonant-cavity InGaAs-InAlAs avalanche photodiodes with gain-bandwidth product of 290 GHz," *IEEE Photon. Technol. Lett.* 11, pp. 1162-1164 (1999).
- [11] A. Banoushi, M.R.Kardan, M. Ataei Naeni, "A circuit model simulation for separate absorption, grading, charge, and multiplication avalanche photodiodes." *Solid-State Electronics*, 49:871-877 (2005)